



GLOBAL JOURNAL OF RESEARCHES IN ENGINEERING: E  
CIVIL AND STRUCTURAL ENGINEERING  
Volume 17 Issue 3 Version 1.0 Year 2017  
Type: Double Blind Peer Reviewed International Research Journal  
Publisher: Global Journals Inc. (USA)  
Online ISSN: 2249-4596 & Print ISSN: 0975-5861

# Prestressed Concrete Inverted Tee Beams with CFRP for Building Structures

By Herish A. Hussein & Zia Razzaq

*Old Dominion University*

**Abstract-** Presented herein is the outcome of a study of prestressed concrete inverted tee beams with carbon fiber reinforced polymer (CFRP) sheets for possible use in building structures. To determine an effective approach for the use of CFRP, nine different retrofitting schemes are investigated for a prestressed beam under quasi-static distributed load to increase flexural strength. The theoretical analysis is based on coupling moment-curvature relations with a central finitedifference formulation. Three different thicknesses of CFRP sheets are studied in both tension and compression and effective retrofitting schemes are identified.

**Keywords:** *CFRP retrofitting, inverted tee beam, prestressed.*

**GJRE-E Classification:** *FOR Code: 090506*



*Strictly as per the compliance and regulations of:*



# Prestressed Concrete Inverted Tee Beams with CFRP for Building Structures

Herish A. Hussein<sup>α</sup> & Zia Razzaq<sup>σ</sup>

**Abstract-** Presented herein is the outcome of a study of prestressed concrete inverted tee beams with carbon fiber reinforced polymer (CFRP) sheets for possible use in building structures. To determine an effective approach for the use of CFRP, nine different retrofitting schemes are investigated for a prestressed beam under quasi-static distributed load to increase flexural strength. The theoretical analysis is based on coupling moment-curvature relations with a central finite-difference formulation. Three different thicknesses of CFRP sheets are studied in both tension and compression and effective retrofitting schemes are identified.

**Keywords:** CFRP retrofitting, inverted tee beam, prestressed.

## I. INTRODUCTION

The effectiveness of CFRP retrofitting when used only in tension zone of prestressed concrete beams has been reported in the past [1-8]. The use of CFRP is beneficial due to its high strength, light weight, non-corrosive nature, and easy installation. [9] Hussein and Razzaq [10] have previously published a study of prestressed concrete box girders with CFRP retrofitting in both tension and compression for use in highway bridges. Presented in this paper is a study of the effectiveness of CFRP sheets in increasing strength and decreasing deflection when used not only in tension but also in compression, or in both tension and compression regions for prestressed concrete inverted tee beams in buildings.

## II. PROBLEM STATEMENT

A prestressed concrete inverted tee beam is shown in Figure 1 carrying a distributed load in addition to its self-weight of 0.45 kips/ft. Figure 2a shows the inverted tee beam cross section without retrofitting. Figures 2b through 2d show the beam cross section retrofitted with single CFRP sheet in tension only, compression only, and simultaneously in both tension and compression, respectively. The CFRP sheet is 1/16 in. thick with a constant width of 11in. The same

retrofitting approaches are repeated with doubling and tripling the CFRP sheets as shown in Figures 2e-2g and 2h-2j, respectively. Each beam has eight 7-wire ASTM Grade 270 1/2 diameter strands in one row as shown.

The following non-linear stress-strain ( $f$  versus  $\epsilon_c$ ) relationship for concrete given by Lin and Burns [11] is adopted for the present study:

$$f_c = f'_c [2(\epsilon_c / \epsilon_o) - (\epsilon_c / \epsilon_o)^2] \quad (1)$$

where  $f'_c$  is the ultimate compression strength at concrete strain  $\epsilon_o$ . The concrete used in this study has an ultimate strength of 8 ksi and a Young's Modulus of 5148 ksi. Furthermore, the CFRP sheet used has an ultimate tensile rupture strength of 260 ksi and a Young's Modulus of 22000 ksi. The stress-strain relation for CFRP in compression is nearly the same as in tension. An elastic-plastic stress-strain relation is adopted for prestressing steel. The problem addressed in this paper is the identification of effective CFRP retrofitting schemes that can practically be utilized for prestressed concrete inverted tee beams in building structures. This is achieved by first developing nonlinear moment-curvature ( $M-\phi$ ) relations for cross sections shown in Figure 2 followed by the formulation of a numerical scheme to predict the load-deflection response of the beam shown in Figure 1 up to collapse.

**Author α:** Research Assistant, Ph.D. Candidate, Department of Civil and Environmental Engineering, Old Dominion University, 115 Kaufman Hall, Norfolk, Virginia, USA. e-mail: hhuss001@odu.edu

**Author σ:** University Professor, Department of Civil and Environmental Engineering, Old Dominion University, 135 Kaufman Hall, Norfolk, Virginia, USA. e-mail: zrazzaq@odu.edu

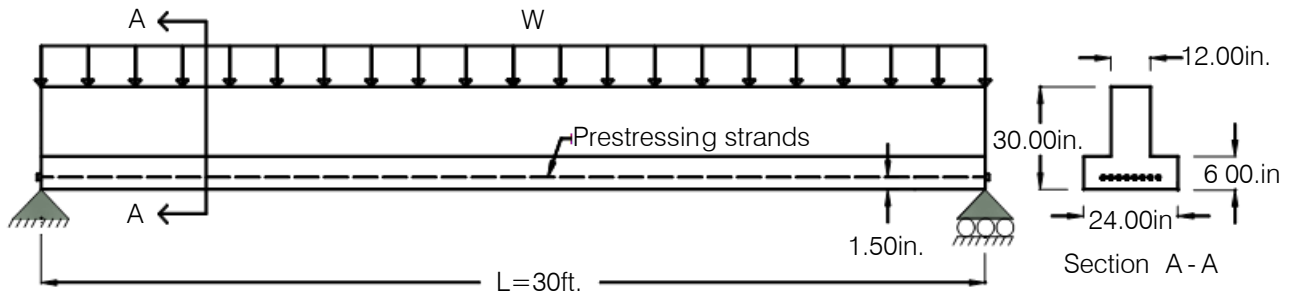


Figure 1: Prestressed concrete inverted tee beam and its cross section

### III. NONLINEAR SOLUTION PROCEDURE

The prestressing strands have a prestress force of 160 kips after prestress losses. Figure 3 shows a typical prestressed beam and strain distribution as well as the associated concrete compressive stress distribution and internal force resultants. The resultant forces are  $C_c$ ,  $T_{ps}$ , and  $T_{CFRP}$  representing, respectively, concrete compression force, prestressing force, and CFRP tensile force. The equation of the resultant force on the compressed concrete and its distance  $X$  from the neutral axis are given by [11]:

$$C_c = b \times c^2 \times f'_c \times \frac{\phi}{\epsilon_c} \left( 1 - \frac{\phi \times c}{3 \epsilon_c} \right) \quad (2)$$

$$X = c \left( \frac{8 \epsilon_c - 3 \phi \times c}{12 \epsilon_c - 4 \phi \times c} \right) \quad (3)$$

where:

$b$  = cross-sectional width at the top,  
 $c$  = neutral axis distance as shown in Figure 3b, and  
 $\phi$  = curvature.

Various loading stages are used to generate the moment-curvature relations. The loading stages are zero external moment, zero strain in concrete at the center of the strands, cracking moment, and the concrete strain reaching 0.001, 0.002, 0.00248, and 0.003 in./in. Elastic bending stress and axial stress equations are used for analysis until the cracking moment is achieved. For the non-linear range, force equilibrium is satisfied after assuming top fiber strain and then iteratively finding the neutral axis location that is, the distance  $c$ . The moment and curvature values are then calculated and used to generate the moment-curvature relations for each beam section shown in Figure 2. For the retrofitting schemes with single, double, and triple CFRP sheets in tension, compression, and in both tension and compression, the moment-curvature ( $M-\phi$ ) relationships developed are presented in Figures 4, 5, and 6, respectively. Next, the moment-curvature relationships are curve-fitted using Excel for each of the beam sections shown in Figure 2. For all of the non-retrofitting and retrofitting schemes, the

following equation is established for the materially linear range:

$$\phi = (0.0005M - 1.2) \times 10^{-5} \quad (4)$$

For the nonlinear portion, the following  $M-\phi$  equations are developed for sections shown in Figures 2a through 2j, respectively:

$$\phi_a = (0.008 \times e^{0.001M}) \times 10^{-5} \quad (5)$$

$$\phi_b = (0.0000006M^2 - 0.005M + 9.54) \times 10^{-5} \quad (6)$$

$$\phi_c = (0.007 \times e^{0.001M}) \times 10^{-5} \quad (7)$$

$$\phi_d = (0.0057M - 32.56) \times 10^{-5} \quad (8)$$

$$\phi_e = (0.0000002M^2 - 0.0003M - 2.61) \times 10^{-5} \quad (9)$$

$$\phi_f = (0.0038 \times e^{0.0011M}) \times 10^{-5} \quad (10)$$

$$\phi_g = (0.0000001M^2 + 0.001M - 4.6) \times 10^{-5} \quad (11)$$

$$\phi_h = (0.0000001M^2 + 0.0006M - 4.26) \times 10^{-5} \quad (12)$$

$$\phi_i = (0.0023 \times e^{0.0011M}) \times 10^{-5} \quad (13)$$

$$\phi_j = (0.0026M - 14.5) \times 10^{-5} \quad (14)$$

It should be noted that the last point on the  $M-\phi$  relations for beam sections 2c, 2f, and 2i are excluded in the above  $M-\phi$  equations. However, the excluded points are separately included when determining the load-deflection relations.

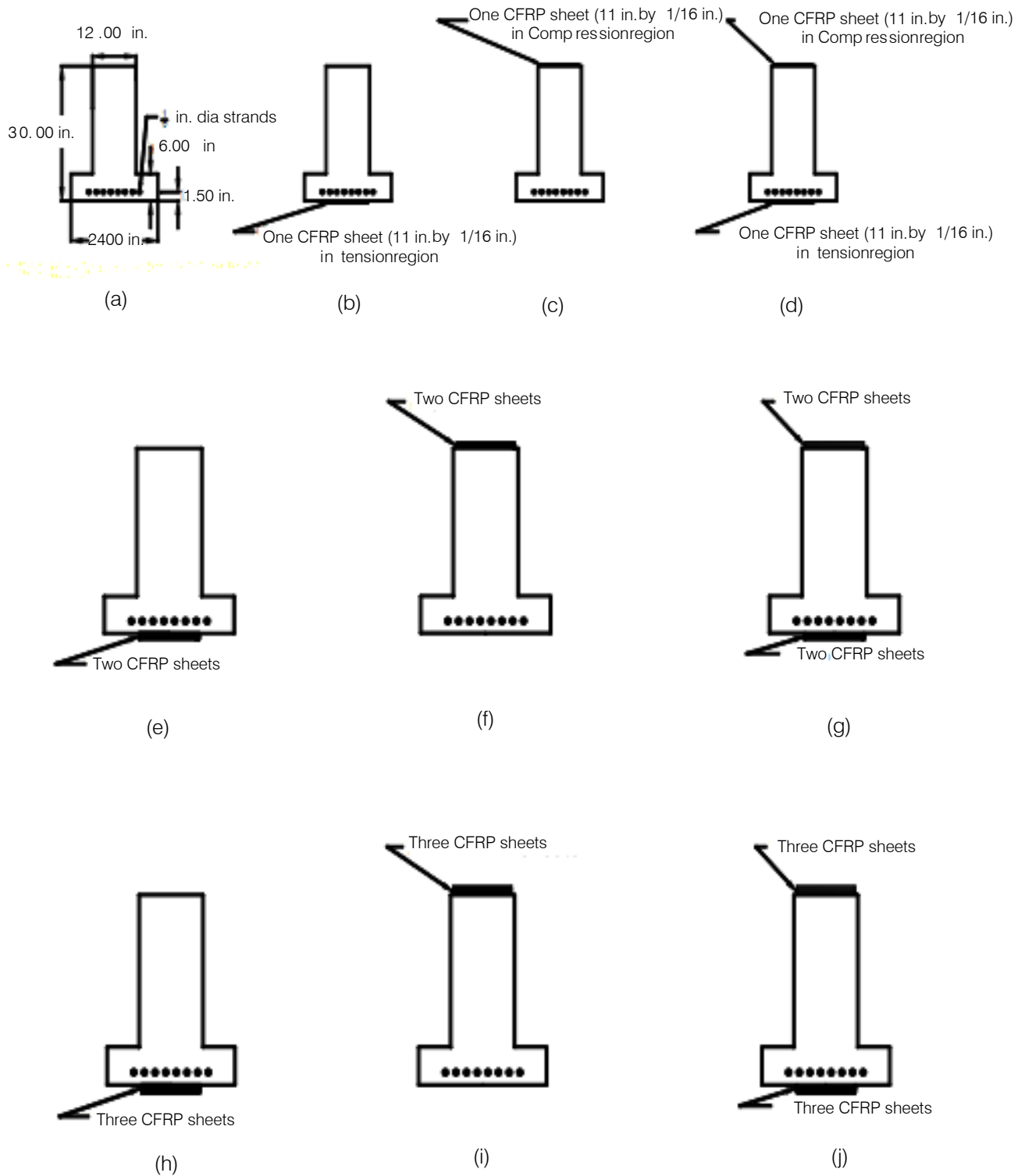


Figure 2: Reference Inverted Tee beam section (a), and various CFRP retrofitting-approach sections (b) through (j)

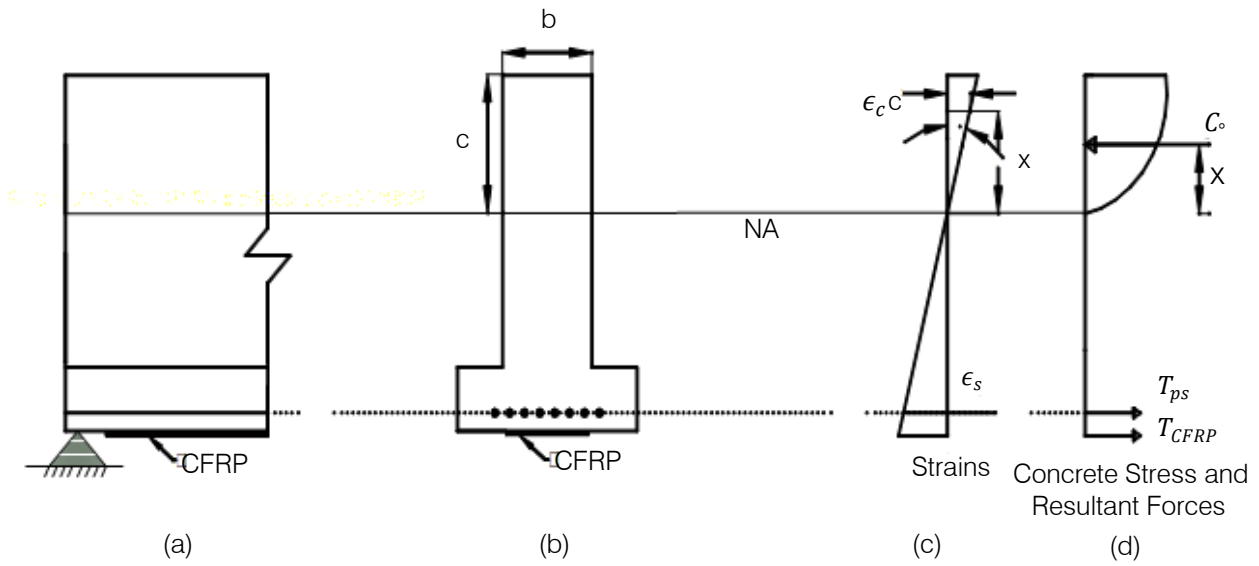


Figure 3: Strain and stress distribution for a simply-supported beam from Figure 2b

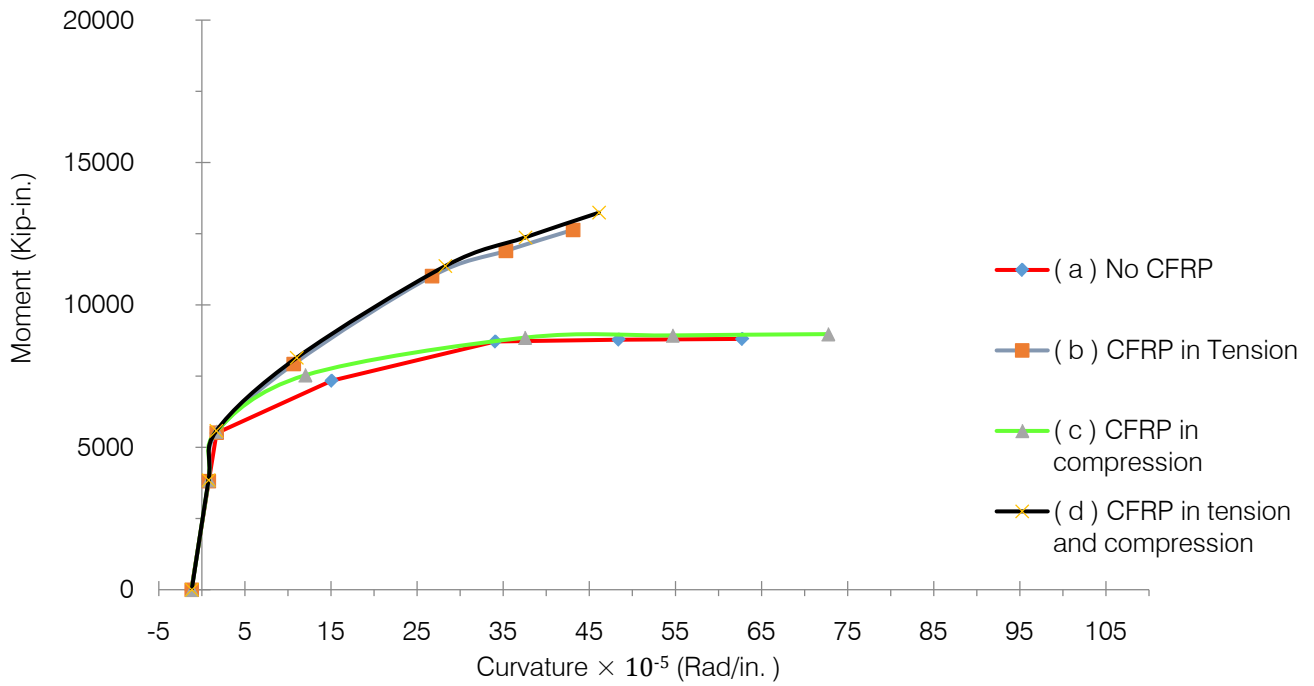


Figure 4: Moment-curvature curves for sections in Figures 2a-2d

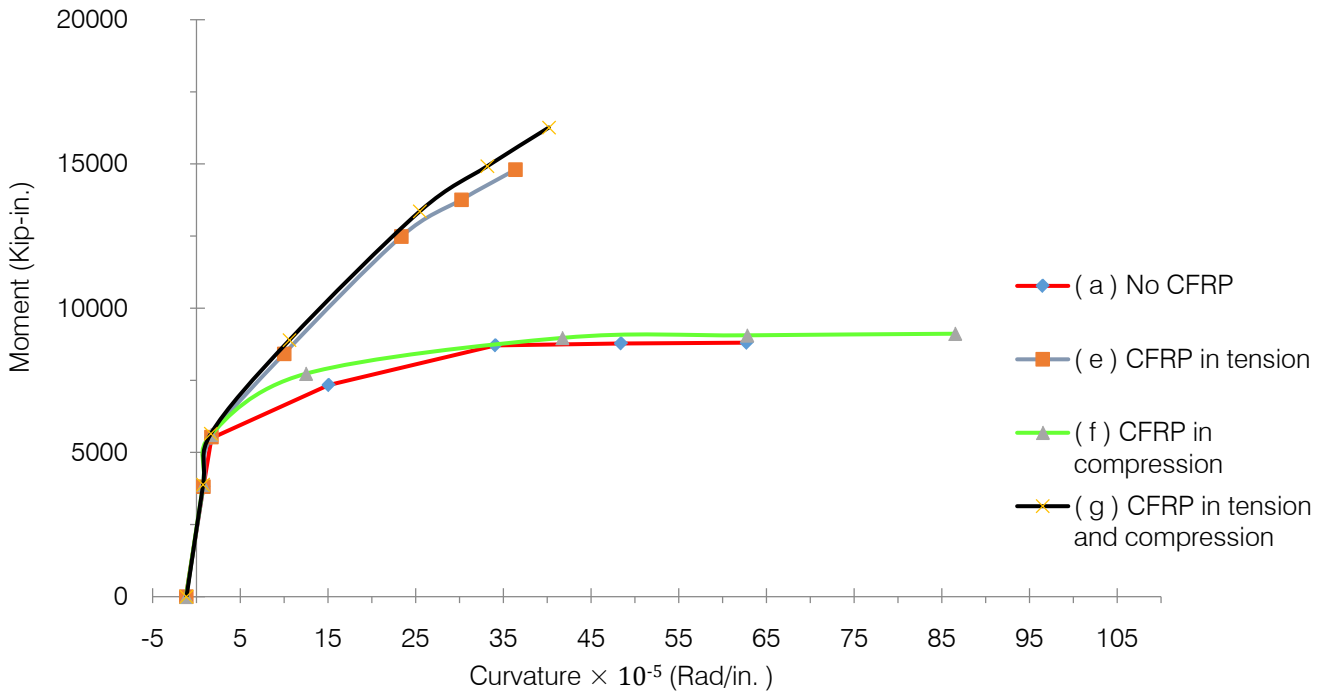


Figure 5: Moment-curvature curves for sections in Figures 2a and 2e-2g

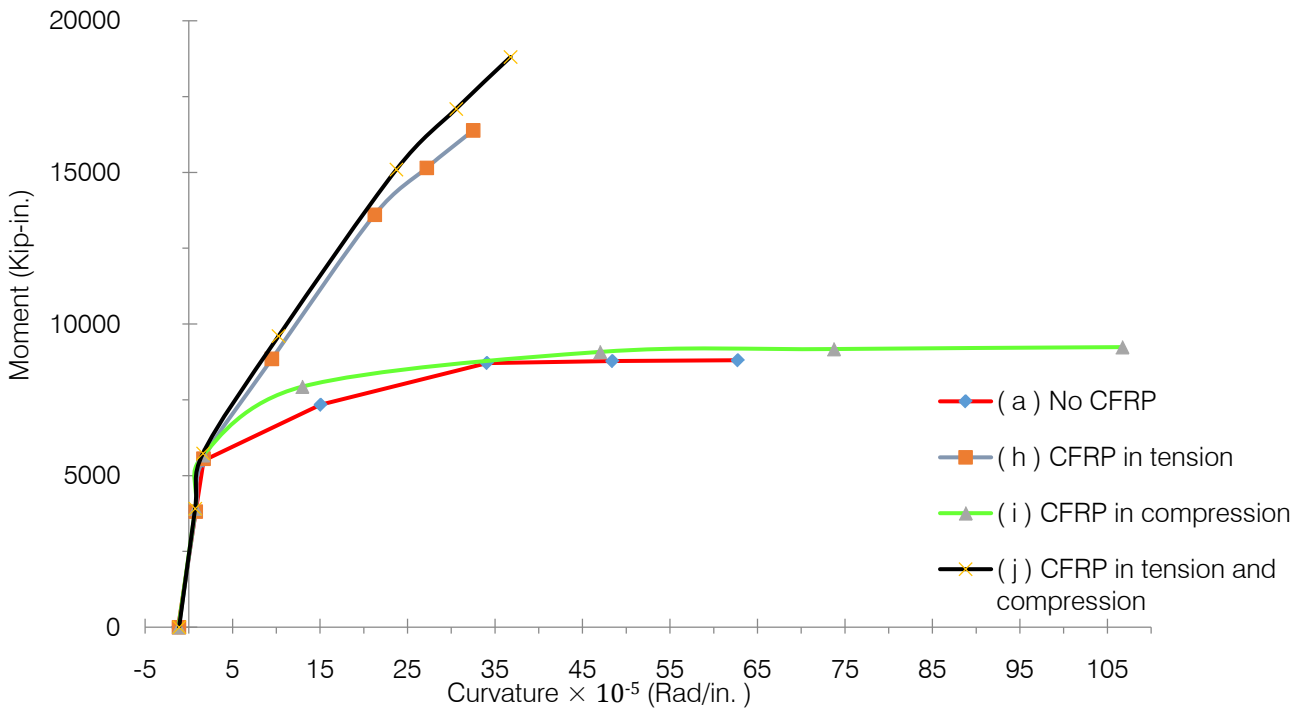


Figure 6: Moment-curvature curves for sections in Figures 2a and 2h-2j

To determine the load-deflection relation for each scheme, the  $M-\phi$  relations are coupled with a central finite-difference algorithm similar to that used by the authors[10]. For the present study, the beam is

divided into ten equal segments ( $h=L/10$ ), and the curvature at any given node  $i$  along the beam length is expressed as[12]:

$$\phi_i = \left(\frac{d^2v}{dz^2}\right)_i = \frac{V_{i-1} - 2V_i + V_{i+1}}{h^2} \quad (15)$$

where:

$V_i$  = deflection at beam node  $i$ .

To calculate the external moment value at any node for various applied loads, the following equation is used:

$$M_z = [(w \times L \times z) - (w \times z^2)]/2 \quad (16)$$

where  $z$  is the beam longitudinal axis.

The nonlinear solution algorithm predicting the beam response are as follows:

1. Specify beam length  $L$ , cross-sectional dimensions, and material properties for concrete, prestressing strands, and CFRP sheets.
2. Divide the beam into  $N$  equal segments along the longitudinal axis associated with node numbers  $i=1, 2, 3, \dots, (N+1)$  over the domain  $0 \leq z \leq L$ .
3. Specify external load  $w = w_1$ .
4. Determine  $M_z$  using Equation 16 at all nodal locations.
5. With  $M_z$  values from step four, determine  $\phi$  using the applicable Equation 4-14.
6. Using Equation 15, generate the following matrix equation to determine nodal deflections,  $V_i$ :

$$[Q]\{V_i\} = \{\phi_i\} \quad (17)$$

7. Solve Equation 17 for the nodal deflection vector  $\{V_i\}$ .

8. Increase  $w$  to  $w_2$  that is, set  $w_2 = w_1 + \Delta w$  and go to step 4.
9. Repeat until the load-carrying capacity is reached corresponding to the collapse condition.

Using the above algorithm, load versus mid-span deflection,  $V_6$ , are predicted and are presented in Figures 7, 8 and 9 for CFRP retrofitted beam sections of 2b-d, 2e-2g, and 2h-2j respectively.

#### IV. NUMERICAL STUDY

Figure 10 compares the maximum moment versus CFRP thickness relations when CFRP is used in tension only to the schemes in which CFRP is used simultaneously in both tension and compression. A comparison of the two curves in this figure reveals that using CFRP in both tension and compression has a greater effect on increasing the moment capacity compared to the scheme involving retrofitting as the tensile side only.

For the presented study, Table 1 presents a summary of the various retrofitting schemes. Presented in this table are the neutral axis location  $c$ , the collapse load  $w_{max}$ , and the increase in  $w_{max}$ ,  $w^*$ .

As can be seen from Table 1, the most effective retrofitting scheme is when three CFRP sheets are simultaneously used in both tension and compression. This scheme (section 2j) resulted in a strength of 2.22 times that obtained with the reference beam (section 2a). The remaining retrofitting schemes are found to be from 1.02 to 1.92 times stronger than the reference beam.

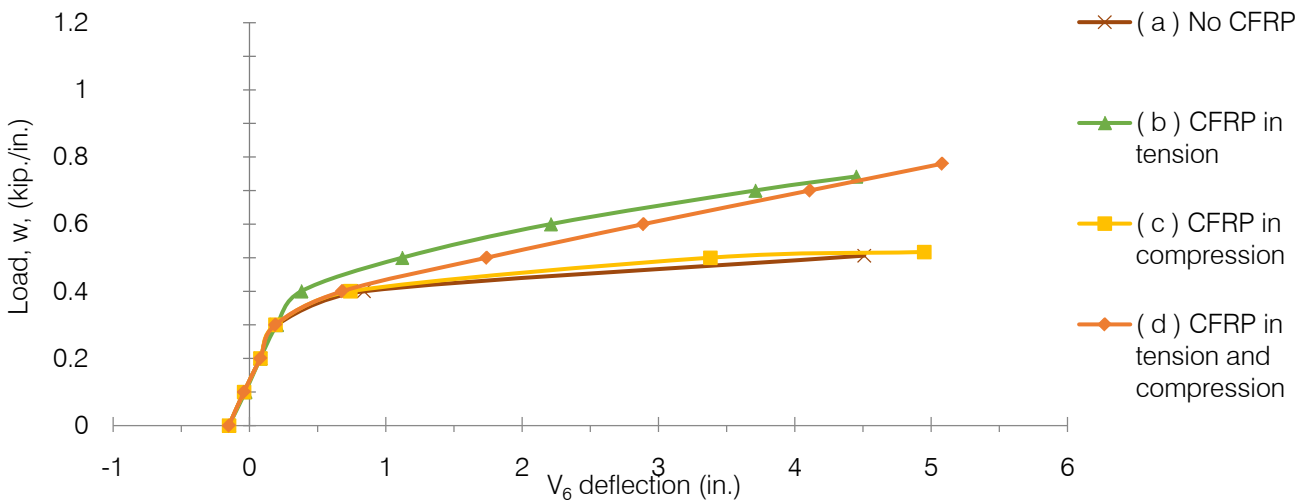


Figure 7: Load-deflection curves for sections in Figures 1a-1d

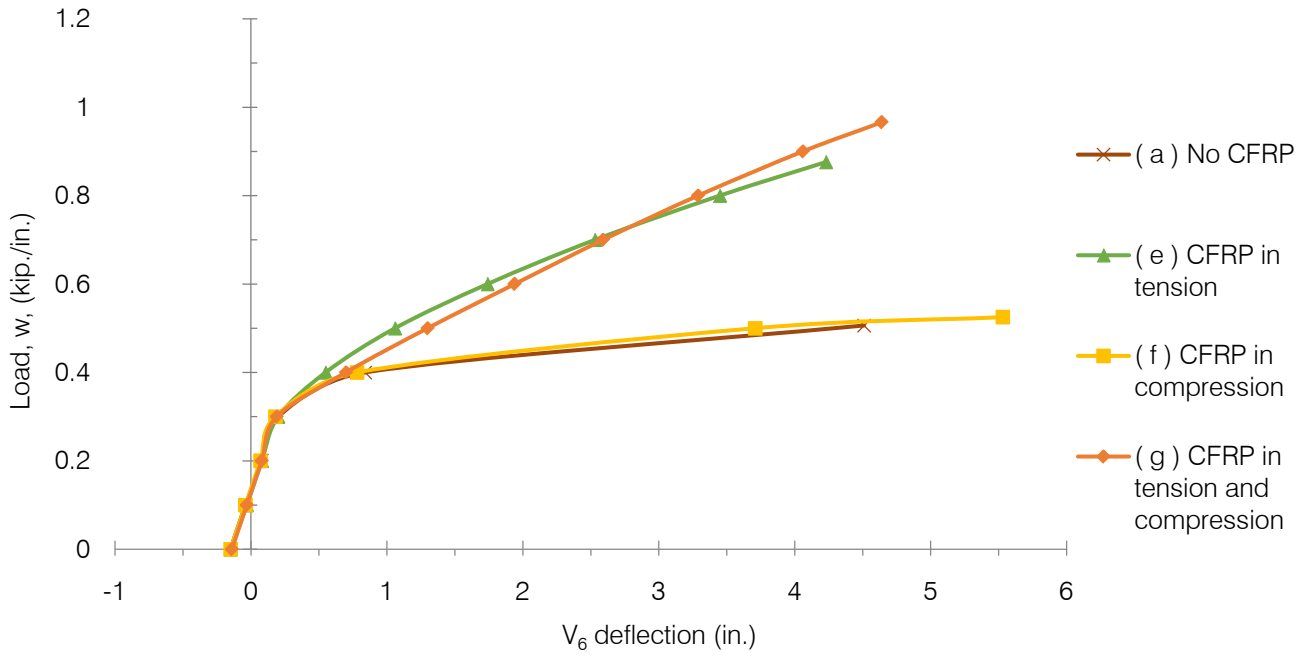


Figure 8: Load-deflection curves for sections in Figures 1a and 1e-1g

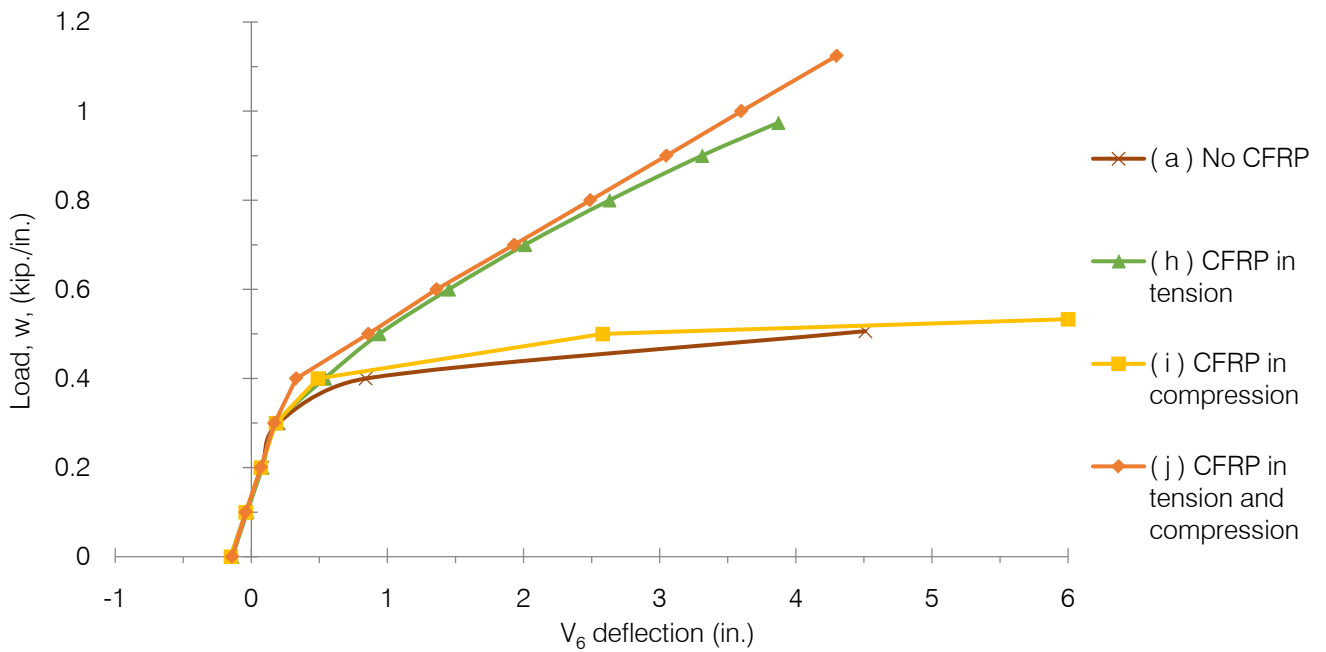


Figure 9: Load-deflection curves for sections in Figures 1a and 1h-1j

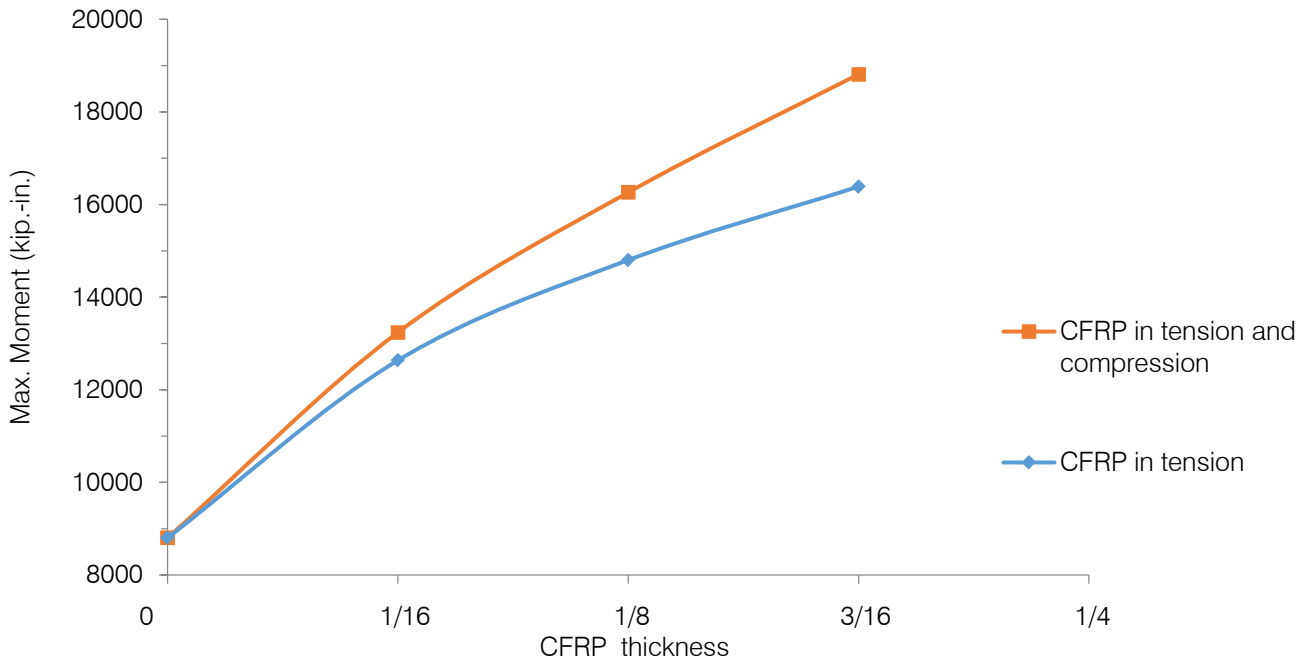


Figure 10: Maximum moment versus CFRP thickness

Table 1: Summary of inverted tee beam results at  $w_{max}$

Section (Figure 2)	c (in.)	$w_{max}$ (kip./in.)	$w^* = w_{max}/0.506$
2a	4.78	0.506	1
2b	6.96	0.742	1.47
2c	4.12	0.517	1.02
2d	6.51	0.780	1.54
2e	8.25	0.876	1.73
2f	3.47	0.525	1.04
2g	7.46	0.966	1.91
2h	9.23	0.974	1.92
2i	2.81	0.533	1.05
2j	8.16	1.124	2.22

### V. CONCLUSIONS

Based on the various CFRP retrofitting schemes studied in this paper, the following principal conclusions are drawn:

1. Developing upon the desired degree of increase in the load-carrying capacity of a prestressed inverted tee beam, are more of the retrofitting schemes considered in this paper can be utilized.
2. The simultaneous use of CFRP retrofitting on both tension and compression is the most effective of the retrofitting schemes considered in this paper.
3. The most effective retrofitting schemes investigated herein result in a very significant reduction in the beam deflection.

The results presented in this study can possibly be implemented in practical CFRP retrofitting issues, related to prestressed inverted tee beams in building structures.

### REFERENCES RÉFÉRENCES REFERENCIAS

1. A. Bennitz, J. W. Schmidt, J. Nilimaa, B. Täljsten, P. Goltermann, and D. L. Ravn, "Reinforced concrete T-beams externally prestressed with unbonded carbon fiber-reinforced polymer tendons," *ACI Structural Journal*, vol. 109, p. 521, 2012.
2. A. Burningham, C. P. Pantelides, and L. D. Reaveley, "Repair of prestressed concrete beams with damaged steel tendons using post-tensioned carbon fiber-reinforced polymer rods," *ACI Structural Journal*, vol. 111, p. 387, 2014.
3. Deifalla and A. Ghobarah, "Effectiveness of the extended CFRP U-jacket for strengthening of RCT-beams under combined torsion and shear," in *The 7th international conference on multi-purpose high rise towers and tall buildings*, Dubai, UA, 2005.
4. R. El-Hacha, R. G. Wight, and M. F. Green, "Prestressed carbon fiber reinforced polymer sheets for strengthening concrete beams at room and low temperatures," *Journal of Composites for Construction*, vol. 8, pp. 3-13, 2004.
5. K. Galal and M. Sekar, "Rehabilitation of RC inverted-T girders using anchored CFRP sheets," *Composites Part B: Engineering*, vol. 39, pp. 604-617, 2008.
6. Y. J. Kim, M. F. Green, and R. G. Wight, "Flexural behaviour of reinforced or prestressed concrete

- beams including strengthening with prestressed carbon fibre reinforced polymer sheets: application of a fracture mechanics approach," Canadian Journal of Civil Engineering, vol. 34, pp. 664-677, 2007.
7. Y. J. Kim, C. Shi, and M. F. Green, "Ductility and cracking behavior of prestressed concrete beams strengthened with prestressed CFRP sheets," Journal of composites for construction, vol. 12, pp. 274-283, 2008.
  8. M. Reza Aram, C. Czaderski, and M. Motavalli, "Effects of gradually anchored prestressed CFRP strips bonded on prestressed concrete beams," Journal of Composites for Construction, vol. 12, pp. 25-34, 2008.
  9. Prince Engineering. (2017, September 25). Carbon Fiber used in Fiber Reinforced Plastic Available: <http://www.build-on-prince.com/carbon-fiber.html#sthash.zXRHeI78.dpbs>
  10. H. A. Hussein and Z. Razzaq, "CFRP Retrofitting Schemes for Prestressed Concrete Box Beams for Highway Bridges," Global Journal of Research In Engineering, 2017.
  11. T. Y. Lin and N. H. Burns, "Design of prestressed concrete structures," 1981.
  12. A. R. Mitchell and D. F. Griffiths, The finite difference method in partial differential equations: John Wiley, 1980.





This page is intentionally left blank